Experimental electronic structure of $Bi_2CaSr_2Cu_2O_{8+\delta}$

F. U. Hillebrecht, J. Fraxedas, L. Ley, H. J. Trodahl, and J. Zaanen
Max-Planck-Institut für Festkörperforschung, Heisenbergstrasse 1, D-7000 Stuttgart 80, Federal Republic of Germany

W. Braun, M. Mast, H. Petersen, and M. Schaible
Berliner Elektronenspeicherring-Gesellschaft für Synchrotronstrahlung m.b.H. (BESSY), Lentzeallee 100, D-1000 Berlin 33, Federal Republic of Germany

L. C. Bourne, P. Pinsukanjana, and A. Zettl
Department of Physics, University of California, Berkeley, California 94720
(Received 16 August 1988)

Highly oriented polycrystalline $Bi_2CaSr_2Cu_2O_{8+\delta}$ has been studied by x-ray photoemission spectroscopy (XPS) to determine the oxidation states of its constituents and the valence electronic structure. Core-level shifts indicate 3+ and 2+ as main oxidation states for Bi and Cu, respectively. The Ca and Sr core levels exhibit pronounced shifts to lower binding energy compared to the metals. The Ca lines show two main components, indicating either inequivalent sites or the presence of a different phase. The XPS and ultraviolet photoemission spectroscopy valence-band spectra show weak but reproducible metallic emission at the Fermi level (E_F) which we ascribe to states originating in the Bi-O planes. The main Cu d–O p band is between 2 and 8 eV below E_F; this is about 1 eV lower than predicted by band-structure calculations. We argue that this is due to electronic correlations tending to increase the anisotropy in the ground-state charge distribution compared to that obtained in local-density-approximation calculations.

I. INTRODUCTION

Reports of high critical superconduction temperatures (T_c) in a new class of materials containing no rare-earth elements have stirred considerable interest recently.[1–4] The absence of the so-called Cu-O chains in $Bi_2(Sr_{1-x}Ca_x)_3Cu_2O_{8+\delta}$ compared to the widely studied $YBa_2Cu_3O_{7-\delta}$ (Y-Ba-Cu-O) has refocused the attention to the Cu-O planes, which are common to both materials, as mainly responsible for the superconductivity.[5–7] Recent band-structure calculations of the Bi compound reveal a novel feature not present in Y-Ba-Cu-O.[8–10] A highly dispersive band of Bi $6p$–O $2p$ states arising from the Bi-O double planes in the structure of $Bi_2(Sr_{1-x}Ca_x)_3Cu_2O_{8+\delta}$ (Ref. 11) with a maximum at $\sim$2 eV above the Fermi level E_F crosses E_F to form an electron pocket about halfway between Γ and Z in the Brillouin zone. This acts to pin the Fermi level via the equilibrium between holes in the Cu-O plane and electrons in the Bi-O plane.

Previous photoemission measurements have—with one exception[12]—failed to observe a metallic Fermi edge in Y-Ba-Cu-O or $La_{2-x}Sr_xCuO_4$.[13,14] This is presumably so because of the highly correlated nature of the corresponding states. The new class of Bi-O states at E_F are expected to be less correlated, and a Fermi edge might therefore be observed.

Here we present a study of highly oriented polycrystals of $Bi_2CaSr_2Cu_2O_{8+\delta}$ by ultraviolet (UPS) and x-ray photoemission (XPS) spectroscopies. Our spectra show indeed reproducibly metallic emission at E_F. Comparison between experimental and calculated densities of states show that electronic correlation appears to be important for this high-T_c superconductor as in other high-T_c superconductors.[4] We discuss this in detail and propose a new renormalized band structure for this high-T_c superconductor.

II. EXPERIMENTAL DETAILS

The crystals of $Bi_2CaSr_2Cu_2O_8$ were grown from a mixture of Bi_2O_3, CuO, $SrCo_3$, and $CaCO_3$ with molar percentages of 22.4%, 32%, 26.9%, and 18.7%, respectively. The powders were mixed in a ball mill with acetone, then placed in a gold crucible, heated to 920 °C for 5 h, and cooled to 820 °C at a rate of 3 °C/h in flowing oxygen. The resulting material is black and cleaves into micaceous sheets. X-ray analysis shows that the c axis is perpendicular to the cleavage plane with a lattice spacing of 3.0 nm, in agreement with the $Bi_2CaSr_2Cu_2O_8$ compound identified by Subramanian *et al.*[7] The midpoint of the superconducting transition is at 82 K.[15]

The XPS experiment was performed using a Surface Science Laboratories X-probe 301 spectrometer. The spectrometer is equipped with a monochromatized Al $K\alpha$ x-ray source providing an x-ray spot of 300×500 μm^2 at the sample and a resolution of 0.7 eV. Fresh sample surfaces were prepared by tearing off thin layers from the sample with double-sided adhesive tape in a vacuum of 10^{-7} torr. Subsequently, the sample was transferred under vacuum to the analyzer chamber held at 10^{-9} torr. For a fast characterization all relevant core lines were measured within half an hour after preparing a fresh surface. Data accumulation for detailed analysis took several

hours during which no change of surface composition was observed. Other samples from the same batch and prepared in the same way were analyzed by UPS in a VG ADES 400 spectrometer in a vacuum of 10^{-10} torr with a resolution of 70 meV.

III. RESULTS

A. Core-level spectra

Except for some variation of the Ca $2p$ line shape to be discussed later, several freshly prepared surfaces yielded identical results. All lines observed between E_F and 1200 eV binding energy were due to the sample constituents, except a C $1s$ line at a binding energy (E_B) of 285.6 eV (all binding energies are referred to E_F) which was always present. This binding energy is characteristic of neutral C as in graphite, or of diamondlike carbon ($E_B \approx 285$ eV)[16] or of C in hydrocarbon, but not of C in carbonates ($E_B \approx 289$ eV).[17] The C $1s$ intensity indicated between 25 and 35 at.% carbon concentration on the surface, but it did not scale with the Ca or Sr concentration. As will be shown in the following, the results on the other core lines are consistent with and fully explained by the superconductor, so that no ligands of the carbon can be identified. Since no bulk foreign phase could be identified in the specimen by x-ray diffraction, we further conclude that the carbonaceous phase is present either in amorphous form and/or concentrated as a thin layer between sheets of the superconducting material at places which are particularly susceptible to cleavage.

Table I shows a typical composition obtained from core-level intensities of a freshly prepared sample. The percentages have been calculated using Scofield's cross sections,[18] the energy dependence of the spectrometer transmission function as specified by the manufacturer ($\propto E_{\rm kin}^{-0.7}$), and an electron mean-free-path scaling as $E_{\rm kin}^{0.5}$, where $E_{\rm kin}$ is the kinetic energy of the photoelectrons.[19] The main sources of error in our determination of composition are the uncertainty in the mean free path, possible deviations of composition near the surface, and the assumption of a uniform depth distribution of the constituents. This assumption is certainly wrong for a material with a pronounced layer structure such as that under consideration here. Nevertheless, there is a rough agreement of the measured surface composition and the composition determined on the basis of x-ray diffraction analysis[4] of the 30.8-Å phase which was reported to be $Bi_2(Ca_{1-x}Sr_x)Sr_2Cu_2O_{8+\delta}$. We note also that the composition of the superconducting phase is still not fully established.[20]

TABLE I. Surface composition in at.% derived from core-level intensities.

Core-level spectra	Measured	Measured without C	Nominal ($\delta=0.5$)
Bi $4f_{7/2}$	11.2	14.8	12.9
Ca $2p_{1/2,3/2}$	3.3	4.4	6.5
Sr $3d_{3/2,5/2}$	8.2	10.8	12.9
Cu $2p_{3/2}$	12.3	16.2	12.9
O $1s$	40.3	53.9	54.8
C $1s$	24.3		

In Fig. 1 x-ray photoemission (XPS) spectra of the Bi $4f$, Ca $2p$, and Sr $3d$ levels are shown together with least-squares fits assuming Gaussians of adjustable width and intensity. The relevant parameters of these fits and of the O $1s$ line of Fig. 2 are collected in Table II. The Bi $4f_{7/2}$ binding energy of 158.5 eV is consistent with a 3+ oxidation state of Bi.[21] Both spin-orbit components show a broadening at the higher-binding-energy side. This could be due to a weak additional line at 1.1 eV higher binding energy arising from Bi in a higher oxidation state — probably 5+ — which would amount to ~7% of the total Bi content. An alternative explanation could be that this line is asymmetrically broadened according to the Doniach-Sunjić line shape,[22] which would imply that the Bi-O planes are metallic.[23] A fit to the Doniach-Sunjić line shape yields an asymmetry parameter $\alpha=0.05$.

The Ca $2p$ spectrum in Fig. 1 can be deconvoluted into three spin-orbit-split doublets at 345.1, 346.1, and 347.1 eV, respectively (referring to the $2p_{3/2}$ lines). The weakest lines may come from a minority phase, but the two major doublets have to be associated with the superconductor. Their relative intensities vary for different cleavages, and appear to be linked to the oxygen content; for a higher oxygen content the 346.1-eV component is enhanced. One possible explanation for the two binding energies may be that Ca occupies some of Sr sites. This would account for the lower-binding-energy component, since the Sr shows a larger shift to lower binding energy than Ca (compared to the metallic binding energies given by Fuggle and Mårtensson[24]). It is worth mentioning in

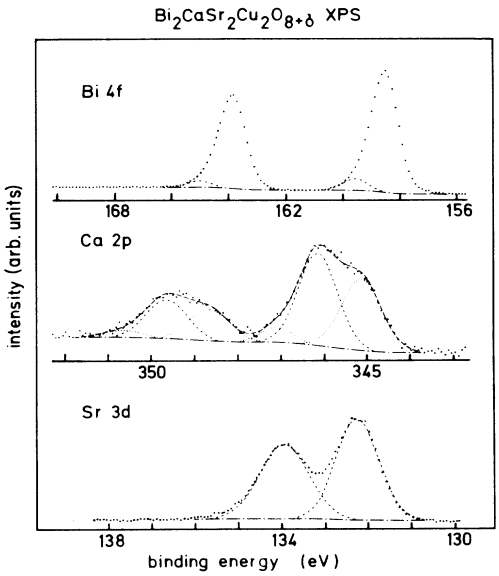

FIG. 1. X-ray photoemission spectra of Bi $4f$, Ca $2p$, and Sr $3d$ core levels. Total resolution is 0.7 eV. The spectra were analyzed by fits to Gaussians. For clarity, the complete fits for Bi and Sr are not shown; they follow the experimental spectra very closely.

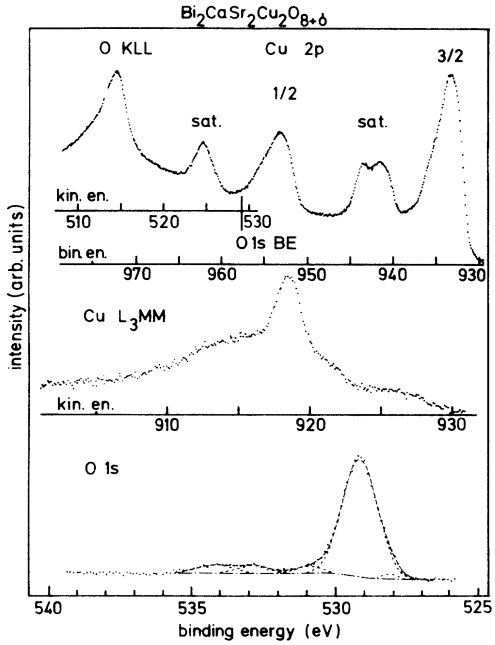

FIG. 2. X-ray photoemission spectra of the Cu $2p$ region, including the O *KLL* Auger spectrum, the x-ray-excited Cu L_3MM Auger spectrum, and the O $1s$ line. Each of the Cu $2p$ spin-orbit components is accompanied by a satellite. The O $1s$ spectrum shows the presence of $\sim 15\%$ of the other phases.

this context that in the structure of Ref. 11 the metal ion in the Sr layer is surrounded by four oxygens. We see from our results that in this coordination the binding energy of the Sr core level is lowered by 2 eV. These oxygen atoms are missing from the Ca planes, so that the Ca core-level binding energy is nearly unaffected. The Ca $2p$ component shifted by 1 eV to lower binding energy is then associated with Ca on Sr sites. It is not uncommon to observe Sr occupying Ca sites,[4] but apparently the reverse situation—Ca occupying Sr sites—is also possible.[25]

The Sr $3d$ spectrum in Fig. 1 consists of a single spin-orbit doublet with peaks at 132.25 and 133.95 eV. These binding energies are 2.0 eV smaller than in metallic Sr.[24] Although shifts to smaller binding energies have been observed for oxides of alkalines and earth alkalines,[26] the shift measured here is remarkably large. We note also that the width of the $3d_{3/2}$ line is significantly larger than the $3d_{5/2}$ width, and the intensity ratio of 1.17 deviates from the expected statistical ratio of 1.5.

Figure 2 shows spectra of the Cu $2p$ region, including the O *KLL* Auger line, O $1s$ core level, and the Cu *LMM* Auger transition. The Cu $2p$ spectrum consists of the two spin-orbit-split main lines, each of which is accompanied by a satellite at -9 eV higher binding energy. The spectrum is similar to that of Cu in other high-T_c superconductors or to that of CuO,[27] i.e., it represents essentially the d^{10} and d^9 final states for the main line and satellite, respectively.[28] The satellite intensity is 29% of the total $2p_{3/2}$ intensity, as in other high-T_c superconductors, but lower than in CuO (31%). The final state associated with the main lines is $2p^5 3d^{10}\underline{L}$, where $\underline{L}$ denotes a ligand (i.e., O $2p$) hole. Because the Cu $3d$ shell is full in this case, there is no multiplet splitting. The width of the main lines is very large (~ 4.2 eV) compared to Cu metal or monovalent Cu compounds, but not dissimilar to what is found in other divalent Cu compounds such as CuO [3.6 eV (Ref. 27)] or the Cu dihalides [2–4 eV (Ref. 28)]. Phonon broadening can be excluded, because this would affect the poorly screened $2p^5 d^9$ states more than the well-screened main lines. On the other hand, a natural explanation for this large width is found in the framework of the Anderson impurity theory for core lines.[29,30] In this picture, the ligand hole ($\underline{L}$) in the screened $2p^5 3p^{10}\underline{L}$ configuration is delocalized in the ligand p band, at least for sufficiently large main-line–satellite splitting. This

TABLE II. Parameters of the core-level spectra shown in Figs. 1 and 2: binding energy (E_B) in eV, weight in % of total, and width (w) in eV. The most-intense components are underlined.

Core-level spectra	E_B (eV)	Weight (%)	w (eV)	E_B (eV)	Weight (%)	w (eV)	E_B (eV)	Weight (%)	w (eV)
Bi $4f_{7/2}$	<u>158.5</u>	<u>52.0</u>	<u>1.10</u>	159.6	4.4	0.93			
$4f_{5/2}$	163.8	41.3	1.15	165.0	2.4	0.93			
Ca $2p_{3/2}$	345.1	28.1	1.09	<u>346.1</u>	<u>35.3</u>	<u>1.05</u>	347.1	4.7	0.86
$2p_{1/2}$	348.7	12.0	1.12	343.7	16.2	1.10	350.7	2.9	1.11
Sr $3d_{5/2}$	<u>132.2</u>	<u>54.0</u>	<u>1.16</u>						
$3d_{3/2}$	134	16.0	1.33						
Cu $2p_{3/2}$	933.1	49	3.9	942.3	20	4.6	9.2[a]	29[b]	
$2p_{1/2}$	953.1	22	4.2	961.9	9	2.8	8.8[a]	29[b]	
O $1s$	528.1	3	1.2	<u>529.2</u>	<u>84</u>	<u>1.4</u>			
$1s$	530.9	4	1.2	532.8	4	1.3	534.2	5	1.2

[a]Separation of main line and satellite.
[b]Satellite intensity in percent of total intensity of the spin-orbit component.

leads to a broadening of the main line essentially proportional to the width of the ligand band. A special feature of the perovskite planes is the presence of 180° Cu—O bonds, maximizing the dispersional width of the Cu d-O p band. Accordingly, the width of this band as determined by band-structure calculations is found to be quite large,[8-10] and this can certainly be held responsible for the observed width of the main lines in the high-T_c compounds. On the other hand, in CuO the bond angles are closer to 90°, leading to a slightly smaller dispersional width[31] and narrower main lines, in agreement with the experimental observations. A theoretical calculation taking into account a realistic density of states will shown whether this picture is sufficient to explain the line shape of the main line in every detail. It may turn out that there are in addition to $3d^{10}\underline{L}$ also $3d^{10}\underline{L}^2$ final states present, leading to the fine structure of the $2p_{3/2}$ main line. For the $2p^5 3d^9$ state the d shell is not full and the satellite line shape is governed by multiplet splitting.[28] This explains the difference in shape and total width of the $\frac{1}{2}$ and $\frac{3}{2}$ satellites. The separation of the main line and satellite is essentially given by the Coulomb interaction between the $2p$ hole and a $3d$ electron, $U_{pd} \cong 9$ eV. The intra-d-shell correlation energy is known[32] to be about 70% of U_{pd}, i.e., $U_{dd} \cong 6$–7 eV. On the basis of these numbers we estimate that a d^8 satellite should occur at ~ 20 eV higher binding energy than the main line. This separation between d^{10} and d^8 final states is somewhat larger than in Ni,[33] where the d^8 satellite has actually been observed. It is clear that a small d^8 satellite cannot be observed with Al $K\alpha$ excitation, because it would be in the region of the Cu $2p_{1/2}$ XPS or the O KLL Auger lines.

The Cu L_3MM Auger spectrum is considerably broadened compared to that of Cu metal,[34] again an effect of the Cu d-O p hybridization.[28] However, the spectrum still shows the typical shape of the d^8 multiplet, of which the ^1G is the dominant state.[34] The energy separation of this line from the peak of the self-convolution of the Cu $3d$ partial density of states yields an upper limit for the Cu d-d Coulomb interaction. We shall return to this point in the discussion of the valence-band results.

The lower part of Fig. 2 shows the O $1s$ XPS spectrum. The dominant line lies at 529.2 eV binding energy. Smaller features which amount to about 12% of the total intensity are seen at higher binding energies up to 534.2 eV. These can be associated, e.g., with carbonate, or small amounts of other phases, while the main line at 529.2 is due to the superconductor. There is also a small contribution at lower binding energy. We cannot determine whether this is an intrinsic feature of the superconductor or caused by a different phase.

B. Valence-band spectra

In Fig. 3 the XPS and UPS valence-band spectra are compared to the total density of states (DOS) calculated within the local-density approximation (LDA). There is some variation in the calculated state densities,[8-10,35] and we show only two of them in the figure. The XPS spectrum shows a broad main band between 1.5 and 7.5 eV

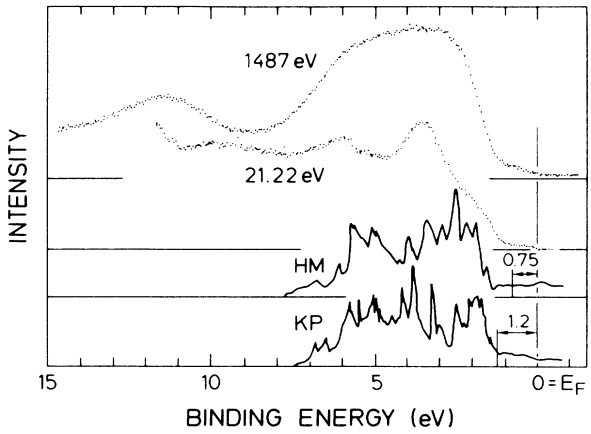

FIG. 3. Valence-band spectrum taken at 300 K with monochromatized Al $K\alpha$ x-ray and He I radiation. The latter one was taken under near-normal emission, with the direction of emission nearly parallel to the c axis, i.e., normal to the layers of the material. No significant differences were observed with different excitation energy (Ne I) at low temperature (30 K) or at up to 50° off-normal emission. Also shown are calculated densities of states reported by Krakauer and Pickett (Ref. 8) and by Hybertsen and Mattheiss (Ref. 9). Note that the calculated spectra are shifted by 1.2 and 0.75 eV to higher binding energy in order to make the most-prominent features in the measured and calculated spectra coincide.

binding energy and a secondary peak centered at 11.4 eV. A comparison of these features with the photoemission data of carbon in its various modifications reveals no similarity.[16,36] We conclude therefore that all structures must be ascribed to the superconductor. This applies also to the UPS spectra, which show the major weight in the same region as the main XPS band, although there are differences in detail. We find structures at 1.6, 3.3, and 5.8 eV below E_F, in agreement with an earlier report.[37] In addition, there is a clear peak at 9.8 eV. These structures depend in position neither on the photon energy nor on the angle of emission. They are therefore identified with maxima in the density of states.

We use the measured valence-band spectrum in connection with the Auger spectrum to deduce the Coulomb correlation energy within the O $2p$ or Cu $3d$ partial densities of states. The underlying relation for the kinetic energy E_K of the Auger electron is[38]

$$E_K(CVV) = E_B(C) - [E_B(V) + E_B(V)] - U_{\text{eff}} .$$

Here C is the initial core hole, V denotes a valence electron, and U_{eff} is the correlation energy. For the sum of the two valence-electron binding energies, one should use the peak of the self-convolution of the appropriate partial densities of states. Since in the superconductor considered here the Cu and O partial density of states are strongly hybridized, we use the experimental XPS valence band. The peak of the self-convolution is at twice the binding energy of the center of gravity of the measured valence-band DOS, i.e., at about 8.4 eV. With this value we obtain for the Cu d-d Coulomb interaction $U_{dd} \cong 5.8$ eV and for the

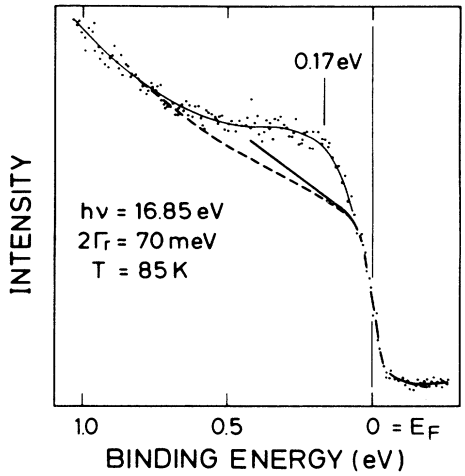

FIG. 4. UPS (Ne I) spectrum of the superconductor taken at 85 K, just above T_c. The solid line is the Fermi edge from a clean Cu surface. The spectra have been corrected for the Ne I satellite emission, assuming a featureless density of states for Cu below E_F. $2\Gamma_r$ is the full width at half maximum of the resolution function.

O p-p Coulomb interaction $U_{pp} \cong 6$ eV. This is similar to values derived for other cuprate superconductors, and also in accord with the estimate obtained above from the Cu core-level satellite. Both for the Cu $3d$ and O $2p$ states the Coulomb correlation energy is comparable to the bandwidth, so that not only the Cu d states, but also the O p states, must be treated as highly correlated.

The higher resolution UPS spectra reproducibly show a Fermi edge of a few percent of the peak emission, and an expansion of this part of the spectrum is shown in Fig. 4. The data in Fig. 4 were taken at 85 K, i.e., just above the onset of superconductivity in our sample. The resolution and position of the Fermi level were determined by fitting the Fermi edge of Cu measured under the same conditions by convoluting the Fermi function with a Gaussian. At 85 K, the sharpness of the Fermi edge is limited to 70 meV by experimental resolution, which allows us to resolve a peak in the DOS at 0.17 eV below E_F. Measurements of the Fermi edge taken down to $T=30$ K showed no changes, i.e., no hint of a superconducting gap.

The peak at 0.17 eV below E_F in Fig. 4 is tentatively ascribed to a local maximum in the density of states due to a flat portion in the highly dispersive Bip–Op bands. Such a feature lies near the M point just above E_F in the calculations of Massidda, Yu, and Freeman[10] and of Krakauer and Pickett.[8] Our experiment would place it just below E_F, in agreement with the band structure of Hybertsen and Mattheis.[9]

IV. DISCUSSION

The comparison of the valence-band spectra with the local-density results reveals several discrepancies, similar to those observed in the other cuprate superconductors.[13,14] First, the 11.4-eV peak is not predicted by the calculations. In our case some Bi $6s$ contribution could be present in this energy region,[38] but because of the small cross section and the low Bi content this cannot explain the observed structure. Furthermore, the same peak is observed in the other superconductors,[13,14] as well as in CuO (Ref. 27) and Cu dihalides (Ref. 28). For Y-Ba-Cu-O there is clear evidence from resonant photoemission that this peak corresponds to a two-hole satellite, or a d^8 lower Hubbard band.[29] We conclude also that the Bi superconductor is characterized by a two-hole satellite, in line with the expectation.

The second discrepancy is that the calculated DOS must be shifted by ~ 1 eV to higher binding energy in order to show a reasonable agreement with the data in the main band region. The agreement is not improved if one takes into account the different energy-dependent cross sections for the partial densities of states.[39] A similar trend has been observed for the other high-T_c superconductors.[13,14] Both the occurrence of the two-hole satellite and this shift result from electronic correlation. In this respect it is illuminating to consider the electronic structure of the Mott-Hubbard insulator NiO. According to LDA band-structure theory the $3d$ states are found in the gap between the occupied O $2p$ bands and unoccupied Ni $4s$ bands.[40] The Fermi energy lies then in a small gap of crystal-field origin in this d-band manifold. However, the electronic structure of NiO turns out to be much better described by an Anderson lattice (or many-band Hubbard) Hamiltonian.[41] The key point is that the d bands are split into a lower and an upper Hubbard band. The lower Hubbard band is located below the bottom of the O $2p$ band and shows up as a satellite in photoemission. The main band is then of predominantly O $2p$ character, although some covalent mixing between the lower Hubbard band and the O $2p$ band returns some $3d$ character into the low-binding-energy region. This leads to a shift of spectral weight to higher energy of the main bands compared to the LDA result.

Some calculations for the photoemission spectra using either the cluster[42] or the impurity approximation[29,43] have been reported for the high-T_c compounds, showing that the d weight is removed from the low-binding-energy region. However, in these calculations the dispersional width of the bands with d character is neglected. It has been argued recently[44] that this may be a poor approximation in the case of high-T_c compounds, both because of the low d-hole count ($\langle n_d \rangle \cong 0.6$) and the previously mentioned 180° Cu–O bonds in the perovskite planes, maximizing the d dispersional width.

Here we would like to suggest an explanation for the discrepancy between the LDA band-structure calculations and the photoemission results which is based on an essentially itinerant ansatz for the electronic structure of the superconductors. We base our model on a recent calculation of the correlation energy in metallic Ni due to Oleś and Stollhoff.[45] Using a local ansatz, these authors found that correlations tend to increase the anisotropy in the charge distribution if there is already a considerable anisotropy present in the charge distribution of the uncorrelated system. In this picture, a contribution to the correlation energy results from the increase of the phase space

for interorbital charge fluctuations if the system is made more anisotropic. The charge anisotropy in elemental Ni stems from the difference in spatial disposition of the d orbitals with e_g and t_{2g} symmetry, respectively. At the center of the Brillouin Zone (BZ) e_g and t_{2g} states are eigenstates with the e_g states lying lower in energy. Away from the BZ center e_g and t_{2g} states mix but in such a way that more of the electrons are in e_g-like states and the holes are in states with predominantly t_{2g} character, yielding the above-mentioned charge anisotropy. Lowering the e_g manifold with respect to t_{2g} will reduce the hybridization and result in the desired increase in the charge anisotropy with the concomitant gain in correlation energy.

The charge distribution in the Cu-O planes of the high-T_c superconductors is also characterized by a considerable anisotropy. The Cu d states with $3z^2-r^2$ and xy, yz, and xz character form a weakly dispersing set of bands that gives rise to the high density of states schematically shown in Fig. 5 as $d_{3z^2-r^2}$.[8-10] The d orbitals with x^2-y^2 symmetry interact with the p orbitals on the neighboring O atoms and form the strongly dispersing band labeled as $d_{x^2-y^2}$ in Fig. 5. It extends beyond E_F and contains the holes which are thus of predominantly $d_{x^2-y^2}$ character. Nevertheless, some $d_{3z^2-r^2}$ character is also mixed in the unoccupied bands.[44] With regard to the findings for the $3d$ metals which have been described above, we expect that electronic correlations within the Cu d manifold will tend to reduce the non-$d_{x^2-y^2}$ charge density above E_F further. The necessary dehybridization is brought about by moving the bands with symmetry different from $d_{x^2-y^2}$ away from E_F. Because the LDA bands giving rise to the high density-of-states region in the occupied density of states are mostly of other than $d_{x^2-y^2}$ character, these —i.e., the bands of $d_{3z^2-r^2}$, d_{xy}, etc., character—have to be moved down, as schematically indicated in the lower part of Fig. 5. We argue that this is the cause for the ~1-eV difference between the LDA calculations and the photoemission results (see Fig. 5). We observe that according to this picture the simple, spin degenerate, two-band Hubbard model containing only the states of $d_{x^2-y^2}$ symmetry[46] may even be a better approximation for the near-ground-state electronic properties of the high-T_c materials than expected from the LDA band structure.[44] To complete our sketch of the electronic structure, it is expected that the $d_{x^2-y^2}$ band is moderately narrowed due to the correlations.[44] At half filling an antiferromagnetic gap is present in the CuO planes at the Fermi energy (see Fig. 5), which probably persists if the system is doped.

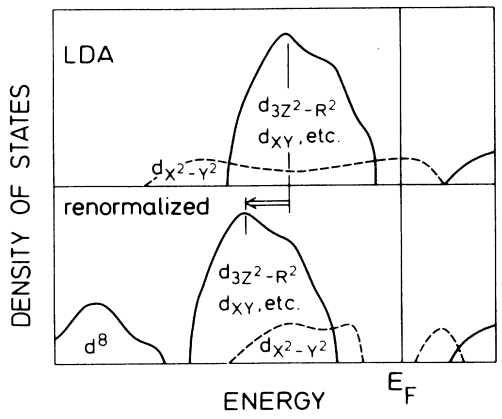

FIG. 5. Schematic density of states of the renormalized bands vs the LDA bands of the high-T_c superconductors at half filling, as discussed in the text.

As mentioned in the Introduction, a Fermi edge is normally not observed in the photoemission spectra of the previously known high-T_c superconductors which do not contain Bi-O planes. All band-structure calculations[8-10] yield a set of highly dispersive bands associated with the Bi-O planes. These bands cross E_F, and we ascribe the photoemission signal observed at E_F to these bands. It is possible, although not certain, that the asymmetric line shape of the Bi $4f$ core lines reflects the metallic character in Bi-O planes. If, however, the Bi $4f$ line shape is caused by two oxidation states, then it is clear that in addition to the Bi 3+ there is about 7% Bi 5+. This has consequences for the structure of the Bi-O layer,[4] which has a strong influence on the band structure and density of states at E_F.[35]

ACKNOWLEDGMENTS

We thank G. Margaritondo for making Ref. 37 available to us prior to publication. Useful discussions with M. Cardona are gratefully acknowledged. One of us (J.F.) would like to thank the Ministerio de Educación y Ciencia (Spain) for financial support. Part of this work was financed by Der Bundesminister für Forschung und Technologie der Bundesrepublik Deutschland.

[1]C. Michel, M. Hervieu, M. M. Borel, A. Grandin, S. Deslandes, J. Provost, and B. Raveau, Z. Phys. B **68**, 421 (1987).

[2]H. Maeda, Y. Tanaka, M. Fukutomi, and T. Asona, Jpn. J. Appl. Phys. Lett. **27**, L209 (1988).

[3]C. W. Chu, J. Bechtold, L. Gao, P. H. Hor, Z. J. Huang, R. L. Meng, Y. Y. Sun, Y. Q. Wang, and Y. Y. Xue, Phys. Rev. Lett. **60**, 941 (1988).

[4]H. G. von Schnering, L. Walz, M. Schwarz, W. Becker, M. Hartweg, T. Popp, B. Hettich, P. Müller, and G. Kämpf, Angew. Chem. Int. Ed. Engl. **27**, 574 (1988).

[5]J. G. Bednorz (unpublished).

[6]R. M. Hazen, L. W. Finger, R. J. Angel, C. T. Prewitt, N. L. Ross, C. G. Hadidiacos, P. J. Heaney, D. R. Veblen, Z. Z. Sheng, A. El Ali, and A. M. Hermann, Phys. Rev. Lett. **60**, 1657 (1988).

[7]M. A. Subramanian, C. C. Torardi, J. C. Calabrese, J. Gopalakrishnan, K. J. Morrissey, T. R. Askew, R. B. Flippen, U. Chowdhry, and A. W. Sleight, Science **239**, 1015 (1988).

[8]H. Krakauer and W. E. Pickett, Phys. Rev. Lett. **60**, 1665 (1988).

[9]M. S. Hybertsen and L. F. Mattheiss, Phys. Rev. Lett. **60**, 1661 (1988).

[10]S. Massidda, J. Yu, and A. J. Freeman, Physica C **152**, 251 (1988).

[11]S. A. Sunshine *et al.*, Phys. Rev. B **38**, 893 (1988).

[12]B. Reihl, T. Riesterer, J. G. Bednorz, and K. A. Müller, Phys. Rev. B **35**, 8804 (1987).
[13]P. D. Johnson, S. L. Qui, F. Garrett, B. Sinkovic, N. V. Smith, R. J. Cava, C. S. Jee, D. Nicols, E. Kaczanowicz, R. E. Salomon, and J. E. Crow, Phys. Rev. B **35**, 8811 (1987); P. Steiner, V. Kinsinger, I. Sander, B. Siegwart, S. Hufner, and C. Politis, Z. Phys. B **67**, 19 (1987); M. Onellion, Y. Chang, D. W. Niles, R. Joynt, G. Margaritondo, N. G. Stoffel, and J. M. Tarascon, Phys. Rev. B **36**, 819 (1987); J. A. Yarmoff, D. R. Clarke, W. Drube, U. O. Karlsson, A. Taleb-Ibrahimi, and F. J. Himpsel, *ibid.* **36**, 3967 (1987).
[14]T. Takahashi, F. Maeda, H. Arai, H. Katayama-Yoshida, Y. Okabe, T. Suzuki, S. Hosoya, A. Fujimori, T. Shidara, T. Koide, T. Miyahara, M. Onoda, S. Shamoto, and M. Sato, Phys. Rev. B **36**, 5686 (1987).
[15]H. F. Goldstein, L. C. Bourne, F. Y. Yu, and A. Zettl (unpublished).
[16]F. R. McFeely, S. P. Kowalczyk, L. Ley, R. G. Cavell, R. A. Pollak, and D. A. Shirley, Phys. Rev. B **9**, 5268 (1974).
[17]U. Gelius, P. F. Hedén, J. Hedman, B. J. Lindberg, R. Manne, R. Nordberg, C. Nordling, and K. Siegbahn, Phys. Scr. **2**, 70 (1970).
[18]J. H. Scofield, J. Electron Spectrosc. Relat. Phenom. **8**, 129 (1976).
[19]C. J. Powell, Surf. Sci. **44**, 29 (1974).
[20]G. S. Grader *et al.*, Phys. Rev. B **38**, 757 (1988); P. A. Morris *et al.*, Appl. Phys. Lett. **53**, 249 (1988).
[21]T. P. Debies and J. W. Rabalais, Chem. Phys. **20**, 277 (1977).
[22]G. K. Wertheim and P. H. Citrin, in *Photoemission in Solids I,* edited by M. Cardona and L. Ley, Topics in Applied Physics, Vol. 26 (Springer-Verlag, Berlin, 1978), p. 197.
[23]J. C. W. Folmer and D. K. G. de Boer, Solid State Commun. **38**, 1135 (1981).
[24]J. C. Fuggle and N. Mårtensson, J. Electron Spectrosc. Relat. Phenom. **21**, 275 (1980).
[25]G. S. Grader, E. M. Gyorgy, P. K. Gallagher, H. M. O'Bryan, D. W. Johnson, Jr., S. Sunshine, S. M. Zahurak, S. Jin, and R. C. Sherwood, Phys. Rev. B **38**, 757 (1988).
[26]G. K. Wertheim, J. Electron Spectrosc. Relat. Phenom. **34**, 309 (1984); G. Ebbinghaus and A. Simon, Chem. Phys. **43**, 117 (1970).
[27]A. Rosencwaig and G. K. Wertheim, J. Electron Spectrosc. Relat. Phenom. **1**, 493 (1973).
[28]G. van der Laan, C. Westra, C. Haas, and G. A. Sawatzky, Phys. Rev. B **23**, 4369 (1981).
[29]O. Gunnarsson and K. Schönhammer, Phys. Rev. B **28**, 4315 (1985).
[30]A. K. McMahan, R. M. Martin, and S. Satpathy, Phys. Rev. B **38**, 6650 (1988).
[31]O. Jepsen (unpublished).
[32]J. Zaanen, C. Westra, and G. A. Sawatzky, Phys. Rev. B **33**, 8060 (1986).
[33]A. Bosch, A. Feil, G. A. Sawatzky, and N. Mårtensson, Solid State Commun. **41**, 355 (1982).
[34]S. P. Kowalczyk, L. Ley, R. A. Pollak, F. R. McFeely, and D. A. Shirley, Phys. Rev. B **8**, 2387 (1973).
[35]F. Herman, R. V. Kasowski, and W. Y. Hsu, Phys. Rev. B **38**, 204 (1988).
[36]D. Marchand, C. Fretigny, M. Laguës, F. Batallan, Ch. Simon, I. Rosenman, and R. Pinchaux, Phys. Rev. B **30**, 4788 (1984).
[37]M. Onellion, Ming Tang, Y. Chang, G. Margaritondo, J. M. Tarascon, P. A. Morris, W. A. Bonner, and N. G. Stoffel, Phys. Rev. B **38**, 881 (1988).
[38]L. Ley, R. Pollak, S. Kowalczyk, and D. A. Shirley, Phys. Lett. **41A**, 429 (1972).
[39]P. Marksteiner, S. Massidda, Jaejun Yu, A. J. Freeman, and J. Redinger, Phys. Rev. B **38**, 5098 (1988).
[40]K. Terakura, T. Oguchi, A. R. Williams, and J. Kuebler, Phys. Rev. B **30**, 4734 (1984).
[41]J. Zaanen and G. A. Sawatzky, Can. J. Phys. **65**, 1262 (1987).
[42]A. Fujimori, E. Takayama-Muromachi, Y. Uchida, and B. Okai, Phys. Rev. B **35**, 8814 (1987).
[43]H. Eskes and G. A. Sawatzky, Phys. Rev. Lett. (to be published).
[44]J. Zaanen *et al.*, Physica C **153–155**, 1636 (1988).
[45]A. M. Oleś and G. Stollhoff, Phys. Rev. B **29**, 314 (1984).
[46]V. J. Emery, Phys. Rev. Lett. **58**, 2794 (1987).